Contribution from the Departments of Chemistry, University of Denver, Denver, Colorado 80208, and University of Colorado at Denver, Denver, Colorado 80202

Metal–Nitroxyl Interactions. 47. EPR Spectra of Two Spin-Labeled Derivatives of EDTA Coordinated to Paramagnetic Metal Ions

Kundalika M. More, Gareth R. Eaton,* and Sandra S. Eaton

Received February 12, 1986

Two spin-labeled derivatives of EDTA were prepared by reaction of one carboxylate group with 2,2,6,6-tetramethyl-4-aminopiperidinyl-1-oxy (product denoted EDTA–NO) or 2,2,6,6-tetramethyl-4-(aminomethyl)piperidinyl-1-oxy (product denoted EDTA–CH_2–NO). Complexes with Cu(II), vanadyl, Ni(II), Cr(III), Fe(III), Mn(II), Dy(III), and Gd(III) were prepared. EPR spectra were obtained in aqueous solution (pH 7) at room temperature and in 1:1 water/propylene glycol at −180 °C. The larger spin–spin interaction between the metal and nitroxyl unpaired electrons in the frozen-solution EPR spectra of the vanadyl, Ni(II), Cr(III), Fe(III), Mn(II), and Gd(III) complexes of EDTA–NO than in the corresponding complexes of EDTA–CH_2–NO was attributed to the large effect of an additional CH_2 group on the exchange interaction. The small difference in the spin–spin interaction between the Cu(II) complexes of EDTA–NO and EDTA–CH_2–NO was attributed to the small effect of the CH_2 group on the dipolar interaction. The rapid relaxation of the metal electrons on Dy(III) caused collapse of the spin–spin splittings even in frozen solution. The relationship between the geometry of the complexes, the number of unpaired electrons on the metal, and the magnitude of the exchange interaction was examined.

Introduction

The exchange interaction between a paramagnetic metal and a nitroxyl radical is a measure of the extent of overlap of the molecular orbitals containing the unpaired electrons. Therefore, the magnitude of the exchange coupling constant, J, is an indication of the bonding pathway between the two paramagnetic sites. In complexes of slowly relaxing transition metals such as Cu(II) and vanadyl the exchange interaction can be measured in fluid solution. However, the relaxation times for many transition metals in fluid solution are sufficiently short that the relaxation of the metal unpaired electrons collapses the spin–spin splitting of the nitroxyl EPR signal. In frozen solution at −180 °C, the metal relaxation times are longer but the EPR spectra are more difficult to interpret because the spin–spin splitting has contributions from both dipolar and exchange interactions.

For metals with $S = {}^1/_2$ it has been shown that measurement of the relative intensity of the half-field transition is a convenient means to separate the exchange and dipolar contributions.[1] In this paper another method is explored for distinguishing between the two contributions to the spin–spin interaction between metals with $S > {}^1/_2$ and nitroxyl radicals. An additional CH_2 group in the linkage between a metal and a nitroxyl radical has been shown to cause a substantial decrease in the exchange interaction.[2,3] However, one CH_2 group causes a rather small increase in the interspin distance for complexes with interspin distances in the range of 7–10 Å (provided the conformations of the molecules with and without the CH_2 group are similar) and therefore causes a small change in the dipolar interaction. Comparison of the magnitude of the spin–spin interaction for two ligands that differ by a single CH_2 group could indicate whether there is a substantial exchange contribution to the spin–spin interaction. Two derivatives of EDTA were therefore prepared that differed by one CH_2 group in the bonding pathway between the metal and the nitroxyl radical, EDTA–NO and EDTA–CH_2–NO. The EPR spectra of complexes of eight paramagnetic metal ions were examined in fluid and frozen solution. This is the most extensive series of paramagnetic metal ions that has been studied with a single spin-labeled ligand.

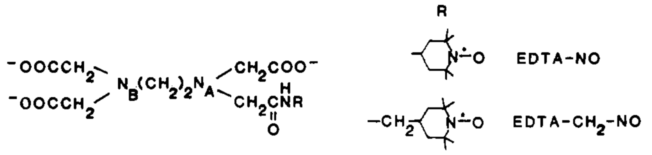

Experimental Section

Physical Measurements. Infrared spectra were obtained in halocarbon mulls or KBr pellets on a Perkin-Elmer 283B spectrometer. Visible spectra were recorded on a Beckman Acta V or a Cary 14 with the On-Line Instruments modification.[4] EPR spectra were obtained on a Varian E9 interfaced to a Varian 620L/103 or to an IBM CS9000 laboratory computer.[5] Spectra were obtained at microwave powers that did not cause saturation and modulation amplitudes that did not distort the line shapes. Spectra at room temperature were obtained on aqueous solutions at pH about 7. Propylene glycol was added to the solutions to obtain good glasses for the frozen-solution spectra. Concentrations were 1×10^{-3}–1×10^{-2} M. In most of the spectra the lines were sufficiently broad that removal of oxygen did not change the line widths. Therefore, spectra were obtained in the presence of oxygen unless otherwise noted. Mass spectra were obtained at the NSF Midwest Center for Mass Spectrometry (Lincoln, NE) or the NIH Mass Spectrometry Research Resource (Denver, CO). A glycerol matrix was used for the FAB spectra. Elemental analyses were performed by Spang Microanalytical Laboratory.

Preparation of EDTA Derivatives. Triethyl *N'*-((((2,2,6,6-Tetramethyl-1-oxy-4-piperidinyl)amino)carbonyl)methyl)ethylenediamine-*N*,*N*,*N'*-triacetate, Et_3–EDTA–NO. Diphenylphosphoryl azide (0.30 g, 1.1 mmol) and triethylamine (0.22 g, 2.2 mmol) were added to a solution of triethyl ethylenediaminetetraacetate[6] (0.376 g, 1.0 mmol) in DMF (10 mL) at 0 °C, and the solution was stirred for 3 h. 4-Amino-2,2,6,6-tetramethylpiperidinyl-1-oxy (0.17 g, 1.0 mmol) was added, and stirring was continued for 4 h at 0 °C and for 15 h at room temperature. Dichloromethane (50 mL) was added. The solution was washed twice with saturated sodium bicarbonate (20 mL) and once with water (30 mL). The solution was dried over anhydrous sodium sulfate, and the solvent was removed to give a red oil. The oil was chromatographed on silica gel. The center of the band that was eluted with 9:1 dichloromethane/methanol was collected. The solvent was removed, yielding 0.40 g (76%) of a yellow oil. IR: 3300 (NH), 1740 (CO, ester), 1660 (CO, amide) cm^{-1}. Mass spectrum: m/e $(M + H)^+$ 530 (EI); $(M + 2\ H)^+$ 531 (FAB). EPR: 1 mol of nitroxyl/mol of compound. Anal. Calcd for $C_{25}H_{45}N_4O_8 \cdot 0.5H_2O$: C, 55.76; H, 8.60; N, 10.40. Found: C, 55.55; H, 8.14; N, 10.22.

Trilithium *N'*-((((2,2,6,6-Tetramethyl-1-oxy-4-piperidinyl)amino)carbonyl)methyl)ethylenediamine-*N*,*N*,*N'*-triacetate, Li_3–EDTA–NO. A solution of lithium hydroxide (72 mg, 3.0 mmol) in water (10 mL) was added to a solution of Et_3–EDTA–NO (0.53 g, 1.0 mmol) in ethanol (5 mL). The mixture was stirred at room temperature for 15 h. The solvent was removed under vacuum, and the residue was recrystallized from methanol/ethyl acetate to give a yellow solid, 0.37 g (80%). IR: 3400

---

* To whom correspondence should be addressed at the University of Denver.

(1) Eaton, S. S.; More, K. M.; Sawant, B. M.; Eaton, G. R. *J. Am. Chem. Soc.* **1983**, *105*, 6560.

(2) More, J. K.; More, K. M.; Eaton, G. R.; Eaton, S. S. *Inorg. Chem.* **1982**, *21*, 2455.

(3) Fielding, L.; More, K. M.; Eaton, G. R.; Eaton, S. S. *J. Am. Chem. Soc.* **1986**, *108*, 618.

(4) The On-Line Instruments System (OLIS) 3920 modification replaces the Cary 14 electronics with stepper motors for the slit and monochromator and controls the system with a Zenith Z-100 microcomputer with 13-bit A/D and D/A converters.

(5) Quine, R. W.; Eaton, G. R.; Eaton, S. S. *J. Magn. Reson.* **1986**, *66*, 164.

(6) Schultz, P. G.; Dervan, P. B. *J. Am. Chem. Soc.* **1983**, *105*, 7748. Taylor, J. S.; Schultz, P. G.; Dervan, P. B. *Tetrahedron* **1984**, *40*, 457.

0020-1669/86/1325-2638$01.50/0

Table I. Preparation of Complexes of EDTA–NO

metal salt	pH for reacn	temp, °C	yield, %	IR ν(CO),[a] cm^{-1}
VOSO$_4$	4	22	75	1620
CrCl$_3$	4	85	80	1635
MnCl$_2$	4	22	78	1590
Fe(OH)$_3$	7	22	[b]	
NiCl$_2$	4	22	82	1600
CuCl$_2$	4	22	80	1605
Gd(OAc)$_3$	4	22	85	1600
DyCl$_3$	4	22	76	1595

[a] In KBr pellet. [b] Not isolated.

(NH), 1600 broad (CO, salt and amide) cm^{-1}.

4-(((*p*-Tolylsulfonyl)oxy)methyl)-2,2,6,6-tetramethylpiperidinyl-1-oxy (I). *p*-Toluenesulfonyl chloride (1.9 g, 10 mmol) was added to a solution of 4-(hydroxymethyl)-2,2,6,6-tetramethylpiperidinyl-1-oxy[7] (1.86 g, 10 mmol) in pyridine (10 mL) and kept at 0 °C overnight. The mixture was poured into crushed ice (50 g). The pink solid was collected by filtration and washed with water (5 mL). The product was crystallized from chloroform/ether. Yield: 3.0 g, 89%. MP: 134 °C. IR: 1170 (OSO$_2$) cm^{-1}.

4-(Azidomethyl)-2,2,6,6-tetramethylpiperidinyl-1-oxy (II). A solution of sodium azide (0.65 g, 10 mmol) in water (2 mL) was added to a solution of I (1.7 g, 5.0 mmol) in DMF (20 mL). The solution was heated at reflux for 4 h. The reaction mixture was diluted with water (20 mL) and extracted with ether (3 × 30 mL). The combined ether layers were dried over anhydrous sodium sulfate, and the solvent was removed under vacuum to give 0.90 g (86%) of a red liquid. IR (neat): 2100 (N$_3$) cm^{-1}.

4-(((Triphenylphosphoranyliden)amino)methyl)-2,2,6,6-tetramethylpiperidinyl-1-oxy (III). Triphenylphosphine (0.79 g, 3.0 mmol) was added to a solution of II (0.63 g, 3.0 mmol) in ether (30 mL), and the mixture was heated at reflux for 1 h. The precipitated product was collected by filtration and recrystallized from chloroform/hexane. Yield: 1.17 g (88%). Mp: 145 °C. IR: 1110 (N=P) cm^{-1}.

4-(Aminomethyl)-2,2,6,6-tetramethylpiperidinyl-1-oxy (IV). A solution of III (0.89 g, 2.0 mmol) in 50% aqueous ethanol (20 mL) was heated at reflux for 10 h. The pH of the solution was adjusted to 4 with 2 N HCl, and the mixture was extracted with chloroform to remove triphenylphosphine oxide. The aqueous phase was neutralized with 10% NaOH and extracted with chloroform (3 × 20 mL). The combined chloroform layers were dried over anhydrous sodium sulfate. Removal of the solvent gave a red oil that crystallized on standing in a refrigerator. Yield: 0.30 g (80%). Mp: 52 °C (lit. 56 °C[8]). The procedures used to prepare I–IV were analogous to those reported in ref 9 for the preparation of 3-(aminomethyl)-2,2,5,5-tetramethylpyrrolinyl-1-oxy.

Triethyl *N'*-(((((2,2,6,6-Tetramethyl-1-oxy-4-piperidinyl)methyl)amino)carbonyl)methyl)ethylenediamine-*N*,*N*,*N'*-triacetate, Et$_3$–EDTA–CH$_2$–NO. The product was prepared from 4-(aminomethyl)-2,2,6,6-tetramethylpiperidinyl-1-oxy and triethyl ethylenediaminetetraacetate[6] by the procedure reported for Et$_3$–EDTA–NO. Yield: 80%. IR: 3300 (NH), 1740 (CO, ester), 1660 (CO, amide) cm^{-1}. Mass spectrum: *m*/*e* (M + 2 H)$^+$ 643 (FAB). EPR: 1 mol of nitroxyl/mol of compound. Anal. Calcd for $C_{26}H_{47}N_4O_8\cdot1.0H_2O$: C, 55.60; H, 8.80; N, 9.97. Found: C, 55.11; H, 8.17; N, 10.43.

Trilithium *N'*-(((((2,2,6,6-Tetramethyl-1-oxy-4-piperidinyl)methyl)amino)carbonyl)methyl)ethylenediamine-*N*,*N*,*N'*-triacetate, Li$_3$–EDTA–CH$_2$–NO. The product was prepared by reaction of lithium hydroxide with Et$_3$–EDTA–CH$_2$–NO by the procedure reported for Li$_3$–EDTA–NO. Yield: 75%. IR: 3400 (NH), 1600 (CO) cm^{-1}.

Preparation of Metal Complexes. The following procedure is typical of the method that was used to prepare the metal complexes. The conditions used for each of the metals are given in Table I.

A solution of CuCl$_2$·2H$_2$O (17 mg, 0.1 mmol) in water (1 mL) was added dropwise to an aqueous solution of Li$_3$–EDTA–NO (46 mg, 0.1 mmol) at pH 4. Dilute LiOH solution was added to maintain the pH at 4. The solution was stirred at room temperature for 10 min, and then the solvent was removed under vacuum. The product was recrystallized from methanol/ethyl acetate. Yield: 0.04 g (80%).

The complexes of EDTA–CH$_2$–NO were prepared similarly. The yields were within 5% of those observed for EDTA–NO, and the carbonyl stretches in the IR region were within 5 cm^{-1} of those observed for the EDTA–NO complexes.

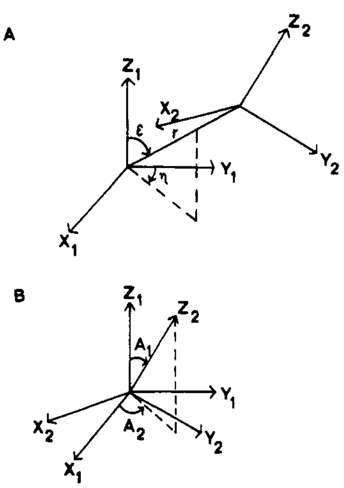

Figure 1. (A) Angles ϵ and η, defining the orientation of the interspin vector relative to the axes of the metal ion (1). (B) Angles A_1 and A_2, defining the orientation of the nitroxyl axes (2) relative to the axes of the metal ion (1). A_1 and A_2 are used in MENO and MANNO, but not in METNO. For each paramagnetic center the *g*, *A*, and ZFS axes were assumed to be coincident.

Computer Simulations. Simulations of the EPR spectra were obtained with the following programs: vanadyl complex of EDTA–NO in fluid solution, CUNO;[10] copper and vanadyl complexes of EDTA–NO in frozen solution, MENO;[11] Mn(II) complexes of EDTA–NO and EDTA–CH$_2$–NO, MANNO.[12] These programs are based on perturbation solutions to the Hamiltonian and include the Zeeman interactions for both metal and nitroxyl, electron–nuclear hyperfine coupling between the unpaired electron(s) on the metal and the nuclear spin of the metal, electron–nuclear hyperfine coupling between the nitroxyl unpaired electron and the nitroxyl nitrogen nuclear spin, isotropic exchange (CUNO) or dipolar and isotropic exchange (MENO and MANNO) interaction between the unpaired electron(s) on the metal and the nitroxyl unpaired electron, and small zero-field splittings (MANNO). The exchange term in the Hamiltonian is $-JS_1\cdot S_2$, and therefore a negative value of J indicates an antiferromagnetic interaction. The angles used to define the relative orientations of the axes and the interspin vector are shown in Figure 1.

To simulate the EPR spectra of the Fe(III) and Cr(III) complexes of EDTA–NO in frozen solution, a program called METNO was written. The large zero-field splittings typically observed for these metals necessitated the use of a diagonalization method. The Hamiltonian included the Zeeman interactions for both metal and nitroxyl, the zero-field splitting for the metal, and dipolar and isotropic exchange interaction between the unpaired electrons on the metal and the nitroxyl. Since most of the isotopes of these metals do not have a nuclear spin, nuclear hyperfine interaction with the metal nucleus was not included in the calculations. Hyperfine coupling to the nuclear spin of the nitroxyl nitrogen also was not included. Thus, the calculations are only applicable to spectra in which the line widths of the nitroxyl lines are greater than the nitroxyl nitrogen hyperfine interaction. Since the nitroxyl *g* values are nearly isotropic, the angles A$_1$ and A$_2$ (Figure 1) that specify the orientation of the nitroxyl axes with respect to the axes of the metal were not defined in these calculations. The energy matrix was solved by using Belford's frequency shift perturbation method.[13,14] This procedure uses diagonalization at one magnetic field (for each orientation of the molecule in the magnetic field) and a perturbation calculation of the field-dependent portion of the energy matrix to determine transition energies and transition probabilities.

Several tests were performed to check the accuracy of METNO. The terms in the matrix describing the electron–electron interaction were compared with the same terms in MENO for a range of interspin distances,

---

(7) Rauckman, E. J.; Rosen, G. M. *Synth. Commun.* **1976**, *8*, 325.

(8) Shapiro, A. B.; Bogach, L. S.; Chumakov, V. M.; Kropacheva, A. A.; Suskina, V. I.; Rozantsev, E. G. *Izv. Akad. Nauk. SSSR, Ser. Khim.* **1975**, 2077.

(9) Hankovsky, H. O.; Hideg, K.; Lex, L. *Synthesis* **1981**, 147.

(10) Eaton, S. S.; DuBois, D. L.; Eaton, G. R. *J. Magn. Reson.* **1978**, *32*, 251.

(11) Eaton, S. S.; More, K. M.; Sawant, B. M.; Boymel, P. M.; Eaton, G. R. *J. Magn. Reson.* **1983**, *52*, 435.

(12) More, K. M.; Eaton, G. R.; Eaton, S. S. *J. Magn. Reson.* **1985**, *63*, 151.

(13) Belford, R. L.; Davis, P. H.; Belford, G. G.; Lenhardt, T. M. *ACS Symp. Ser.* **1974**, *No. 5*, 40.

(14) Scullane, M. I.; White, L. K.; Chasteen, N. D. *J. Magn. Reson.* **1982**, *47*, 383.

r, and exchange interactions, *J*. Calculated transition energies, transition probabilities, and spectra for metal spin $^1/_2$ were compared with values calculated with MENO when the electron–nuclear hyperfine coupling constants were set equal to zero. Results obtained for metal spin $^5/_2$ and small zero-field splitting were compared with those obtained from MANNO when the electron–nuclear hyperfine coupling constants were set equal to zero. Spectra were also calculated with several different diagonalization fields. Except when energy levels of interest cross, the calculated transition fields appeared to be accurate within a few gauss for the cases examined.

Spectra were calculated for 740–1720 orientations of the molecule with respect to the magnetic field. Typical calculations on a VAX 780 computer required 1–2 min for metal $S = {}^1/_2$ and 30–40 min for metal $S = {}^5/_2$.

Results and Discussion

Two spin-labeled derivatives of EDTA were prepared by reaction of an amino-substituted nitroxyl radical with one carboxylic acid of EDTA to form an amide linkage. In EDTA–NO the nitroxyl ring was attached directly to the amide. In EDTA–CH_2–NO there was a CH_2 group between the nitroxyl ring and the amide. The two ligands were reacted with paramagnetic metal ions in aqueous solution. Since many metal ions catalyze the cleavage of amide linkages,[15] some EDTA and free nitroxyl were formed during the reactions to form the metal complexes of EDTA–NO and EDTA–CH_2–NO. Most of the reactions were done at pH 4 to minimize the cleavage reactions. Lower pH caused destruction of the nitroxyl radical. Recrystallization of the spin-labeled complexes removed most of the nitroxyl that had been cleaved off but left a contamination with the corresponding EDTA complex. The EPR spectra of the copper, vanadyl, and nitroxyl signals indicated that about 75% of the product was the spin-labeled EDTA complex and 25% was the EDTA complex. The double integral of the signal near $g = 2$ accounted for all of the nitroxyl in the metal complexes. The sharp signal from nitroxyl that was not interacting with the metals was a few percent.

Numerous X-ray crystal structures of complexes of monoprotonated $HEDTA^-$ have shown that it functions as a pentadentate ligand.[16,17] The protonated carboxyl group and associated CH_2 group are pointed away from the metal coordination sphere, and H_2O occupies vacant coordination sites on the metal. Molecular models indicate that conversion of the free carboxylate group to a spin-labeled amide does not require changes in the metal coordination sphere. It therefore seems reasonable to assume that the geometries of the coordination spheres of the spin-labeled complexes are similar to those observed for the complexes of $HEDTA^-$. The similarities in the EPR parameters for the metals in the $HEDTA^-$ complexes and the spin-labeled complexes support this proposal. Similar structures have been assumed for other monosubstituted EDTA metal complexes.[6] In this conformation the amide carbonyl and the nitroxyl are at substantial distances from the metal, so exchange interaction between the metal and the nitroxyl would be through N_A and the CH_2 group rather than by direct interaction. The metal–nitroxyl distances obtained from the EPR spectra of the complexes discussed below are consistent with this orientation of the spin-labeled carboxylate.

Metals with $S = {}^1/_2$, Copper(II) and Vanadyl. In a 1:1 mixture of water (pH 7) and propylene glycol the frozen-solution EPR spectrum of the copper(II) complex of EDTA contained two components in an approximately 1:2 ratio. Component **1** had g_x and g_y = about 2.07, $g_z = 2.33$, A_x and A_y less than line widths, and $A_z = 0.0154$ cm^{-1}. Component **2** had g_x and g_y = about 2.06, $g_z = 2.29$, A_x and A_y less than line widths, and $A_z = 0.0156$ cm^{-1}. At pH 4, only component **1** was observed. It had previously been proposed that at pH 7 the copper(II) complex of EDTA existed as a 1:2 mixture of $Cu(H_2EDTA)(H_2O)$ containing pentadentate EDTA and a coordinated water molecule and $Cu(HEDTA)^-$ containing hexadentate EDTA.[18,19] The hexadentate form is unlikely to persist at low pH. Therefore, the pH dependence of the EPR spectra was consistent with the assignment of components **1** and **2** to the complexes containing pentadentate EDTA and hexadentate EDTA, respectively. The *g* values for component **1** was similar to those reported in a single-crystal EPR study of $Cu(H_2EDTA)(H_2O)$, $g_x = 2.0688$, $g_y = 2.0580$, $g_z = 2.341$.[20] A single-crystal X-ray study of $Cu(H_2EDTA)(H_2O)$ showed that the coordinated water was in an equatorial position, one protonated carboxylate group was weakly coordinated in an axial position, and the second protonated carboxylate group was attached to the nitrogen that was bound weakly in the second axial position.[21]

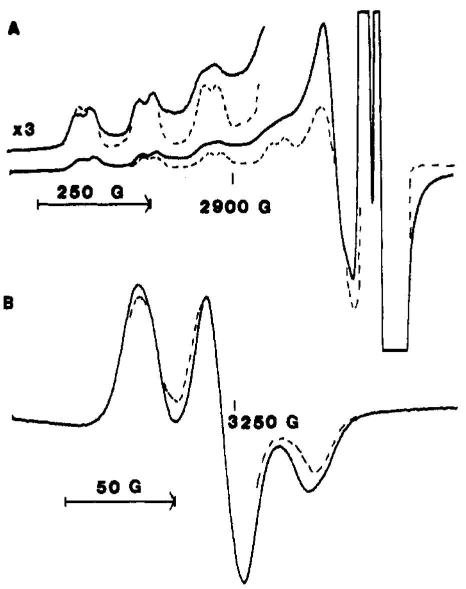

Figure 2. X-Band (9.101 GHz) EPR spectra of Cu(HEDTA–NO)(H_2O) in frozen solution at −180 °C: (A) 1000-G scan obtained with 0.63-G modulation amplitude and 1.0-mW microwave power; (B) 200-G scan obtained with 0.5-G modulation amplitude and 0.2-mW microwave power. The dotted lines indicate regions in which the simulated spectra do not overlay the experimental curves. Values of the parameters used in the simulations are as follows. Copper: $g_x = 2.065$, $g_y = 2.070$, $g_z = 2.330$ $A_x = 0.0010$ cm^{-1} $A_y = 0.0010$ cm^{-1} $A_z = 0.0155$ cm^{-1}. Nitroxyl: $g_x = 2.0089$, $g_y = 2.0066$, $g_z = 2.0025$, $A_x = 0.0004$ cm^{-1}, $A_y = 0.0005$ cm^{-1}, $A_z = 0.0035$ cm^{-1}, $A_1 = 75°$, $A_2 = 45°$. Interaction: $J = 0.0$ cm^{-1}, $r = 11.0$ Å, $\epsilon = 0°$, $\eta = 0°$.

The EPR spectrum of the copper(II) complex of EDTA–NO had *g* values similar to those for $Cu(H_2EDTA)(H_2O)$. A single component was observed at pH 4 and 7. It is therefore proposed that the complex was Cu(HEDTA–NO)(H_2O). By analogy with the structure of $Cu(H_2EDTA)(H_2O)$, N_A was in an axial position, the water was in an equatorial position, and the protonated carboxylate group was in the second axial position. The EPR spectrum of Cu(HEDTA–NO)(H_2O) in frozen solution is shown in Figure 2. The small distortion of the nitroxyl signal due to interaction with the unpaired electron on the copper(II) indicated that the spin–spin interaction was weak. The splitting of the parallel lines in the copper spectrum was larger than the splittings of the copper perpendicular lines, which indicated that the interspin vector was closer to the copper *z* axis than to the *xy* plane, which is consistent with the coordination geometry proposed above. The intensity of the half-field transition was strongly concentration-dependent, which indicated that intermolecular contributions were larger than intramolecular contributions and that the interspin distance was relatively long. The spectra were simulated with a dipolar interaction (11.0 Å) and no exchange interaction. Since the unpaired spin density was in the *xy* plane[20] and the bonding pathway between the nitrogen in the *xy* plane (N_B) and the

---

(15) Groves, J. T.; Chambers, R. R., Jr. *J. Am. Chem. Soc.* **1984**, *106*, 630 and references therein.
(16) Nuttall, R. H.; Stalker, D. M. *Talanta*, **1977**, *24*, 355.
(17) Porai-Koshits, M. A.; Polynova, T. N. *Koord. Khim.* **1984**, *10*, 725; *Sov. J. Coord. Chem.* (*Engl. Transl.*) **1984**, *10*, 395.
(18) Oakes, J.; Smith, E. G. *J. Chem. Soc., Faraday Trans. 1* **1983**, *79*, 543.
(19) Higginson, W. C. E.; Samuel, B. *J. Chem. Soc. A* **1970**, 1579.
(20) Hathaway, B. J.; Bew, M. J.; Billings, D. E.; Dudley, R. J.; Nicholls, P. *J. Chem. Soc. A* **1969**, 2312.
(21) Stephens, F. S. *J. Chem. Soc. A* **1969**, 1723.

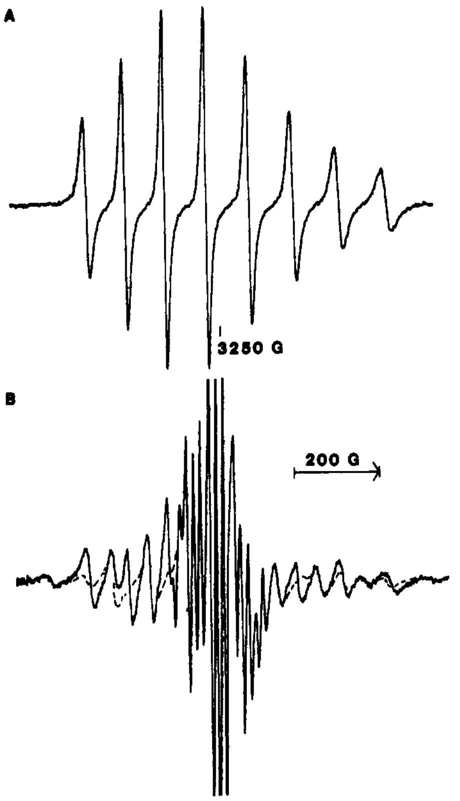

Figure 3. X-Band (9.101 GHz) EPR spectra (1000 G) in fluid solution at room temperature: (A) spectrum of $VO(EDTA)^{2-}$ obtained with 2-G modulation amplitude and 5-mW microwave power, simulated with g = 1.981 and A_{VO} = 0.0096 cm^{-1}; (B) spectrum of $VO(EDTA\text{-}NO)^-$ obtained with 2.5-G modulation amplitude and 5-mW microwave power. The dotted lines indicate the regions in which the simulated spectrum does not overlay the experimental curve. The simulation does not include the contributions from $VO(EDTA)^{2-}$ or nitroxyl that was not interacting with the vanadyl. Values of the parameters used in the simulation are as follows. Vanadyl: g = 1.981, A = 0.0096 cm^{-1}. Nitroxyl: g = 2.0059, A = 0.00152 cm^{-1}, J = 0.0140 cm^{-1}.

nitroxyl on the axial nitrogen (N_A) included 3 CH_2 groups, the absence of a substantial exchange interaction was reasonable.

In frozen solution the EPR spectrum of $Cu(HEDTA\text{-}CH_2\text{-}NO)(H_2O)$ was similar to that of $Cu(HEDTA\text{-}NO)(H_2O)$ although with slightly smaller spin–spin splittings. The additional CH_2 group caused a small increase in the interspin distance (r = about 11.5 Å). In fluid solution the nitroxyl signals in both copper complexes had line widths of about 20 G, but there was no resolved spin–spin splitting. Since rapid molecular tumbling averages dipolar splittings to nearly zero but does not eliminate isotropic exchange splittings, the absence of resolved splitting in the fluid-solution spectra was consistent with the conclusion that the exchange contribution to the spin–spin interaction was small in these copper(II) complexes.

A single-crystal X-ray study of Ba(VO(EDTA)) showed that the EDTA was pentadentate and that the nitrogen to which the free carboxylate was attached was coordinated in the equatorial plane (cis to the V═O bond).[22] By analogy it is proposed that $VO(EDTA\text{-}NO)^-$ had N_A coordinated in the equatorial plane. The EPR spectrum of $VO(EDTA\text{-}NO)^-$ in fluid solution is shown in Figure 3B. Superimposed on the spectrum of $VO(EDTA)^{2-}$ (Figure 3A) were additional signals due to spin–spin interaction between the metal and nitroxyl unpaired electrons in $VO(EDTA\text{-}NO)^-$. This spectrum is similar to those observed previously for other spin-labeled vanadyl complexes.[23] The simulated

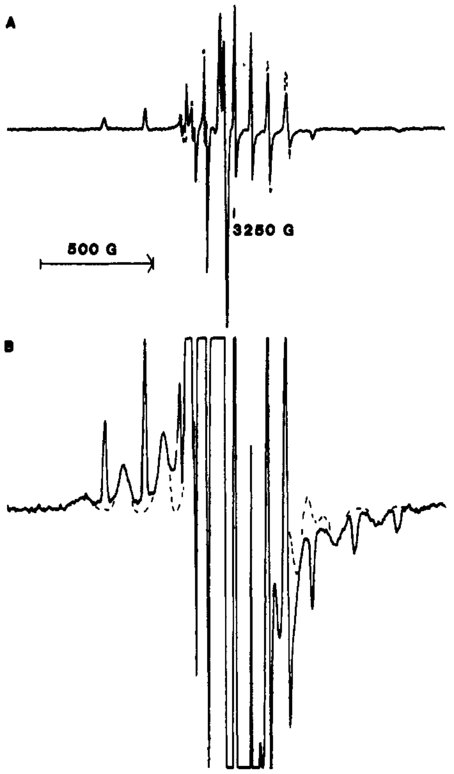

Figure 4. X-Band (9.101 GHz) EPR spectra (2000 G) in frozen solution at −180 °C. (A) Spectrum of $VO(EDTA)^{2-}$ obtained with 0.5-G modulation amplitude and 0.2-mW microwave power. The dotted lines indicate the regions in which the simulated spectrum does not overlay the experimental curve. Values of the parameters used in the simulation: g_x = 1.991, g_y = 1.984, g_z = 1.950, A_x = 0.0061 cm^{-1}, A_y = 0.0060 cm^{-1}, A_z = 0.0170 cm^{-1}. (B) Spectrum of $VO(EDTA\text{-}NO)^-$ obtained with 4-G modulation amplitude and 0.5-mW microwave power. The dotted lines indicate the regions in which the simulated spectrum does not overlay the experimental curve. The contribution to the spectrum from $VO(EDTA)^{2-}$ (sharp lines between the broad lines) was not included in the simulation. The values of the parameters used in the simulation were as follows. Vanadyl: same as in part A. Nitroxyl: same as in Figure 2B except A_1 = 30° and A_2 = 30°. Interaction: J = −0.0140 cm^{-1}, r = 9.0 Å, ϵ = 70°, η = 0°.

spectrum was obtained with J = 0.0140 cm^{-1}. The g value and A value for $VO(EDTA)^{2-}$ are typical of the values commonly observed for vanadyl, so the unpaired electron was probably in the d_{xy} orbital that was oriented between the bonds to the ligands in the equatorial plane as in other vanadyl complexes.[23] In most cases where electron–electron exchange interactions of this magnitude have been observed, there was an overlap of the metal orbital containing the unpaired electron with an orbital on a ligand atom. It therefore seems surprising to have a substantial exchange interaction between the nitroxyl and vanadyl unpaired electrons when the orbital containing the metal unpaired electron is nominally orthogonal to the orbitals of N_A. It is proposed that the symmetry of the complex is sufficiently low that there is nonzero overlap of the metal d_{xy} orbital with the orbitals on the coordinated nitrogen N_A.

In the frozen-solution EPR spectrum of $VO(EDTA\text{-}NO)^-$ (Figure 4B) the wings of the spectra showed spin–spin splitting of the vanadyl parallel lines. The magnitude of the splitting was similar to that observed in fluid solution, which indicated that the exchange interaction was still present in addition to a dipolar contribution. It was assumed that the interspin vector was near the equatorial plane. There was substantial overlap of the nitroxyl signals with the vanadyl perpendicular lines from $VO(EDTA\text{-}NO)^-$ and from $VO(EDTA)^{2-}$, so the only conclusion that could be drawn from the central portion of the spectrum was that the nitroxyl lines were strongly effected by interaction with the vanadyl unpaired electron. Since detailed information could not be obtained from the perpendicular lines, it can only be said that the

---

(22) Nesterova, Ya. M.; Anan'eva, N. N.; Polynova, T. N.; Porai-Koshits, M. A.; Pechurova, N. I. *Dokl. Akad. Nauk SSSR* **1977**, *237*, 350; *Dokl. Chem.* (*Engl. Transl.*) **1977**, *237*, 660.

(23) Sawant, B. M.; Shroyer, A. L. W.; Eaton, G. R.; Eaton, S. S. *Inorg. Chem.* **1982**, *21*, 1093.

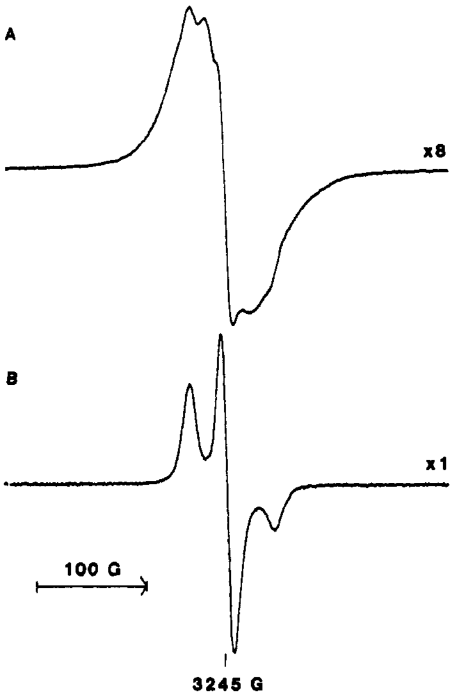

Figure 5. X-Band (9.101 GHz) EPR spectra (400 G) in frozen solution at −180 °C: (A) spectrum of $Ni(HEDTA\text{-}NO)(H_2O)$ obtained with 1.6-G modulation amplitude and 0.2-mW microwave power; (B) spectrum of $Ni(HEDTA\text{-}CH_2\text{-}NO)(H_2O)$ obtained with 0.5-G modulation amplitude and 0.2-mW microwave power. The relative amplification for the spectra was corrected for the differences in spectrometer settings and sample concentrations.

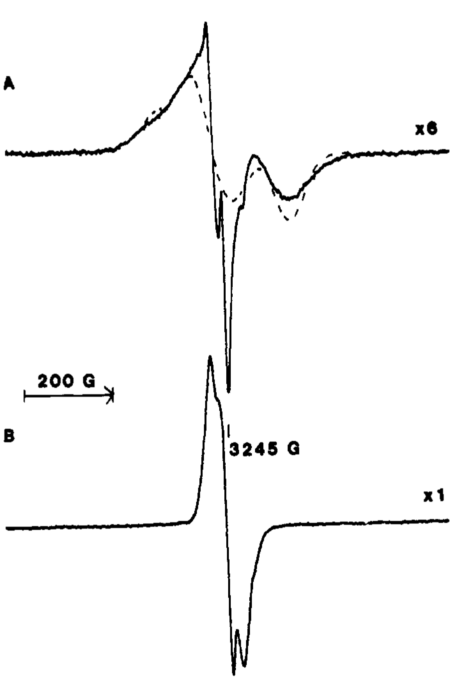

Figure 6. X-Band (9.101 GHz) EPR spectra (1000 G) in frozen solution at −180 °C. (A) Spectrum of the nitroxyl signals in $Cr(EDTA\text{-}NO)$ obtained with 1.25-G modulation amplitude and 0.5-mW microwave power. The dotted line indicates the regions in which the simulated spectrum does not overlay the experimental curve. The values of the parameters used in the simulation were as follows. Chromium $g = 2.0$, $D = 0.5$ cm^{-1}, $E/D = 0.1$. Nitroxyl: g values as in Figure 2B. Interaction: $J = -0.006$ cm^{-1}, $r = 7.5$ Å, $\epsilon = 70°$, $\eta = 10°$. (B) Spectrum of the nitroxyl signals in $Cr(EDTA\text{-}CH_2\text{-}NO)$ obtained with 2-G modulation amplitude and 0.5-mW microwave power. The relative amplification for the spectra was corrected for differences in spectrometer settings and sample concentrations.

spectra were consistent with a value of J = about ±0.0140 cm^{-1} and r = about 8–10 Å.

In fluid solution the EPR spectrum of $VO(EDTA\text{-}CH_2\text{-}NO)^-$ consisted of superimposed vanadyl and nitroxyl lines that indicated negligible exchange interaction between the two unpaired electrons. In frozen solution the dipolar interaction caused broadening of the spectra, but the lines were not sufficiently well resolved to permit a determination of the interspin distance. Thus, the additional CH_2 group in $VO(EDTA\text{-}CH_2\text{-}NO)^-$ caused a dramatic decrease in the exchange interaction compared with that which was observed in $VO(EDTA\text{-}NO)^-$.

Thus, the data for the Cu(II) and vanadyl complexes indicated that in these complexes the additional CH_2 group in the metal–nitroxyl linkage had a much larger impact on the exchange interaction than on the dipolar interaction.

Metal with $S = 1$, Nickel(II). Crystals of $Ni(H_2EDTA)(H_2O)$ are isomorphous with the analogous copper(II) complex.[24] Several studies in fluid solution have indicated that near pH 7 the nickel complex existed as a mixture of pentadentate and hexadentate EDTA complexes[18,19,25] analogous to the copper(II) complexes. It is therefore proposed that the nickel(II) complex of EDTA–NO was $Ni(HEDTA\text{-}NO)(H_2O)$ with a structure similar to that of the copper complex. The EPR spectrum of $Ni(HEDTA\text{-}NO)(H_2O)$ in frozen solution is shown in Figure 5A. The nitroxyl signal was strongly distorted by interaction with the unpaired electrons on the nickel(II). Due to the short T_1 of the nickel unpaired electrons, the splitting of the nitroxyl signal due to spin–spin interaction was probably partially collapsed by rapid relaxation of the metal electrons, so a simulation was not attempted. Spectra at lower temperatures will be needed to determine the magnitude of the spin–spin interaction in this sample.

The nitroxyl signals in the frozen-solution EPR spectrum of $Ni(HEDTA\text{-}CH_2\text{-}NO)(H_2O)$ (Figure 5B) showed much less indication of interaction with the nickel than the nitroxyl signals in the spectrum of $Ni(HEDTA\text{-}NO)(H_2O)$ (Figure 5A). Thus, the additional CH_2 group had a large effect on the magnitude of the spin–spin interaction for the nickel(II) complexes. This is analogous to the large effect of the additional CH_2 group on the exchange interaction in the vanadyl complexes and unlike the small effect of the CH_2 group on the dipolar interaction in the copper(II) complexes. It is therefore proposed that there was a substantial exchange contribution to the spin–spin interaction in $Ni(HEDTA\text{-}NO)(H_2O)$. Since one of the unpaired electrons is expected to be in the d_{z^2} orbital directed toward the axial nitrogen (N_A), it is reasonable to expect significant exchange interaction in this complex.

In fluid solution the nitroxyl signals in $Ni(HEDTA\text{-}NO)(H_2O)$ and $Ni(HEDTA\text{-}CH_2\text{-}NO)(H_2O)$ were sharp three-line patterns. The nickel relaxation rate at room temperature was probably so fast that the metal unpaired electron was effectively decoupled from the nitroxyl unpaired electron.

Metal with $S = {}^3/_2$, Chromium(III). In fluid solution between pH 3.5 and 6.5, deuterium NMR indicated that the chromium complex of EDTA was $Cr(EDTA)^-$ containing hexadentate EDTA and that at higher or lower pH the EDTA was pentadentate and 1 mol of hydroxide or water was coordinated.[26] A single-crystal X-ray structure of $Cr(HEDTA)(H_2O)$ found a distorted octahedral coordination sphere made up of a pentadentate EDTA and a coordinated water molecule.[27] It is therefore proposed that the Cr(III) complex of EDTA–NO is $Cr(EDTA\text{-}NO)(H_2O)$.

The EPR spectrum of $Cr(HEDTA)(H_2O)$ in frozen solution had broad features at g = about 2.0, 3.42, and 4.48, which indicated that the value of D was >0.3 cm^{-1}.[28] For Cr(III) the value of D is typically <1.0 cm^{-1},[28,29] so D was assumed to be

---

(24) Smith, G. S.; Hoard, J. L. *J. Am. Chem. Soc.* **1959**, *81*, 556.
(25) Grant, M. W.; Dodgen, H. W.; Hunt, J. P. *J. Am. Chem. Soc.* **1971**, *93*, 6828.
(26) Wheeler, W. D.; Legg, J. I. *Inorg. Chem.* **1984**, *23*, 3798.
(27) Gerdom, L. E.; Baenzinger, N. A.; Goff, H. M. *Inorg. Chem.* **1981**, *20*, 1606.
(28) Bencini, A.; Gatteschi, D. *Transition Met. Chem.* (*N.Y.*) **1982**, *8*, 1.
(29) Carlin, R. L.; Burriel, R.; Pons, J.; Casabo, J. *Inorg. Chem.* **1983**, *22*, 2832.

between 0.3 and 1.0 cm^{-1}. The nitroxyl region of the EPR spectrum of Cr(EDTA–NO)(H_2O) in frozen solution is shown in Figure 6A. The sharp signals in the center of the spectrum were due to a small amount of nitroxyl that was not interacting with chromium(III). The spin–spin interaction between the chromium(III) and the nitroxyl unpaired electrons caused the signal from the nitroxyl in the complex to be spread over several hundred gauss. The simulated spectra were insensitive to the magnitude of D when D was in the range of 0.3–1.0 cm^{-1} but were dependent on the relative signs of J and D. The observed spectrum had greater intensity to low field of $g = 2$ than to high field of $g = 2$. This pattern was reproduced by $J/D < 0$ but not by $J/D > 0$. A similar fit to the experimental data was obtained for $J = -0.006$ cm^{-1} and $r = 7.5$ Å or $J = +0.008$ cm^{-1} and $r = 10.0$ Å. Thus, it was not possible to determine the sign of J or D. The chromium signals were sufficiently broad that the effect of the spin–spin interaction on the chromium signals could not be determined.

The spectrum of the nitroxyl signals in Cr(EDTA–CH_2–NO)(H_2O) in frozen solution is shown in Figure 6B. The spectrum could not be simulated with METNO because the nitroxyl nitrogen hyperfine splitting could not be neglected. Although the nitroxyl spectrum was broadened by spin–spin interaction between the nitroxyl and chromium unpaired electrons, the magnitude of the spin–spin interaction was substantially smaller than in Cr(EDTA–NO)(H_2O). It is therefore proposed that the exchange interaction in this complex was much smaller than for the EDTA–NO complex due to the additional CH_2 group in the linkage between the metal and the nitroxyl.

In fluid solution the EPR spectra of the nitroxyl signals in Cr(EDTA–NO)(H_2O) and Cr(EDTA–CH_2–NO)(H_2O) had line widths of 14 and 2 G, respectively. By analogy with the spectra of spin-labeled complexes of slowly relaxing transition metals such as Cu(II), it might have been anticipated that the exchange interaction between Cr(III) and nitroxyl in Cr(EDTA–NO)(H_2O) would have caused resolved spin–spin splitting in the fluid-solution spectrum. However, NMR studies have indicated that T_1 for Cr(III) complexes in fluid solution is of the order of 3×10^{-10} s (21 kG) to 3×10^{-9} s (63 kG).[30] Since T_1 decreases at lower field, the shorter values are more likely to be relevant to EPR experiments. Values of T_1 in the range of 10^{-9}–10^{-10} s are short enough to cause partial collapse of the splitting of the spin–spin splitting but leave substantial broadening of the nitroxyl signal, as observed in the spectrum of Cr(EDTA–NO)(H_2O). The sharp nitroxyl signals in the room-temperature spectrum of Cr(EDTA–CH_2–NO)(H_2O) reflect the averaging of the dipolar splitting by molecular tumbling and the rapid relaxation of the unpaired electron on the metal.

Metals with $S = {}^5/_2$, Iron(III), Manganese(II), and Dysprosium(III). Single-crystal X-ray studies have been reported for Fe(HEDTA)(H_2O) in which the EDTA is pentadentate and the iron is 6-coordinate[31] and for Fe(EDTA)(H_2O)$^-$ in which the EDTA is hexadentate and the iron is 7-coordinate.[32] It has been proposed on the basis of visible and Mössbauer spectra that the species in fluid solution are Fe(HEDTA)$(H_2O)_2$ and Fe(EDTA)(H_2O)$^-$, both of which are 7-coordinate.[33] NMR studies indicated that in the pH range 4–9 the only species present in solution was Fe(EDTA)(H_2O)$^-$.[18,34] Since the visible spectra of the iron(III) complexes of the spin-labeled EDTA derivatives agreed well with the spectra of Fe(EDTA)(H_2O)$^-$, it is probable that the complexes are Fe(EDTA–NO)$(H_2O)_2$ and the iron is 7-coordinate. Analysis of the Q-band EPR spectrum of Fe(EDTA)$^-$ doped into Co(EDTA)$^-$ gave $D = 0.83$ cm^{-1} and $E = 0.31$.[35] Inclusion of higher order terms in the zero-field splitting (ZFS) improved the fit to the experimental data but did not have a large impact on the value of D.[36] Although the ZFS in frozen solution is likely to be different from that in the single crystal and is likely to be different for Fe(EDTA–NO)$(H_2O)_2$ than for Fe(EDTA)$^-$, these data give an indication of the magnitude of ZFS that is expected for this class of compounds.

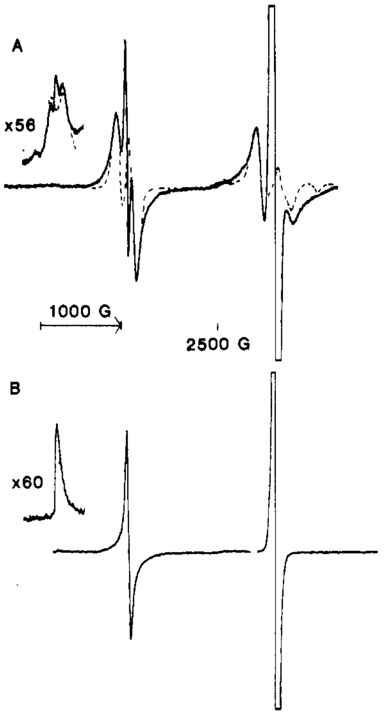

Figure 7. X-Band (9.101 GHz) EPR spectra (4000 G) in frozen solution at −180 °C. (A) Spectrum of Fe(EDTA–NO) obtained with 4-G modulation amplitude and 5-mW microwave power. The dotted lines indicate regions in which the simulated spectrum does not overlay the experimental curve. The values of the parameters used in the simulation were as follows. Iron: $g = 2.0$, $D = -0.60$ cm^{-1}, $E/D = 0.333$. Nitroxyl: g values as in Figure 2B. Interaction: $J = 0.013$ cm^{-1}, $r = 7.5$ Å, $\epsilon = 90°$, $\eta = 10°$. (B) Spectrum of Fe(EDTA–CH_2–NO) obtained with 4-G modulation amplitude and 5-mW microwave power.

In frozen solution the EPR spectrum of Fe(EDTA–NO)$(H_2O)_2$ showed spin–spin splitting of both the iron signals and the nitroxyl signal (Figure 7A). The sample also contained small amounts of Fe(EDTA)(H_2O)$^-$ and nitroxyl that was not interacting with iron(III). These impurities gave sharp signals that were readily distinguished from the signals in the complex. The simulations of the spectra were insensitive to the magnitude of D in the range 0.3–1.0 cm^{-1}. In the simulations of the iron signals, changes in the signs of J, D, and E could be compensated by changes in the angles ϵ and η. For example, the set $J = +0.013$ cm^{-1}, $D = -0.5$ cm^{-1}, $E/D = 0.33$, $\epsilon = 0$, and $\eta = 0$ was equivalent to $J = +0.013$ cm^{-1}, $D = 0.5$ cm^{-1}, $E/D = 0.33$, $\epsilon = 90$, and $\eta = 90$. This was an indication of internal consistency in the program. However, agreement of the simulations of the nitroxyl signals with the experimental data was better for $J/D < 0$ than for $J/D > 0$.

The EPR spectrum of Fe(EDTA–CH_2–NO)$(H_2O)_2$ in frozen solution is shown in Figure 7B. The iron and nitroxyl signals were broadened by the spin–spin interaction, but splittings were not resolved. The iron signals were at the g values for Fe(EDTA)(H_2O)$^-$. These signals are characteristic of $D > 0.3$ cm^{-1} and E/D = about ${}^1/_3$.[14,35] Comparison of the spectra in Figure 7A,B indicated that the spin–spin interaction was much weaker for Fe(EDTA–CH_2–NO)$(H_2O)_2$ than for Fe(EDTA–NO)$(H_2O)_2$. Most of that decrease is attributed to a decrease in the exchange interaction.

In fluid solution the nitroxyl signals in the EPR spectra of Fe(EDTA–NO)$(H_2O)_2$ and Fe(EDTA–CH_2–NO)$(H_2O)_2$ had

---

(30) Hexem, J. G.; Edlund, U.; Levy, G. C. *J. Chem. Phys.* **1976**, *64*, 936.

(31) Hoard, J. L.; Kennard, C. H. L.; Smith, G. S. *Inorg. Chem.* **1963**, *2*, 1316.

(32) Lind, M. D.; Hamor, M. J.; Hamor, T. A.; Hoard, J. L. *Inorg. Chem.* **1964**, *3*, 34.

(33) Garbett, K.; Lang, G.; Williams, R. J. P. *J. Chem. Soc. A* **1971**, 3433.

(34) Block, J.; Navon, G. *J. Inorg. Nucl. Chem.* **1980**, *42*, 693.

(35) Aasa, R. *J. Chem. Phys.* **1970**, *52*, 3919.

(36) McGarvin, D. G.; Tennant, W. C. *J. Magn. Reson.* **1985**, *62*, 357.

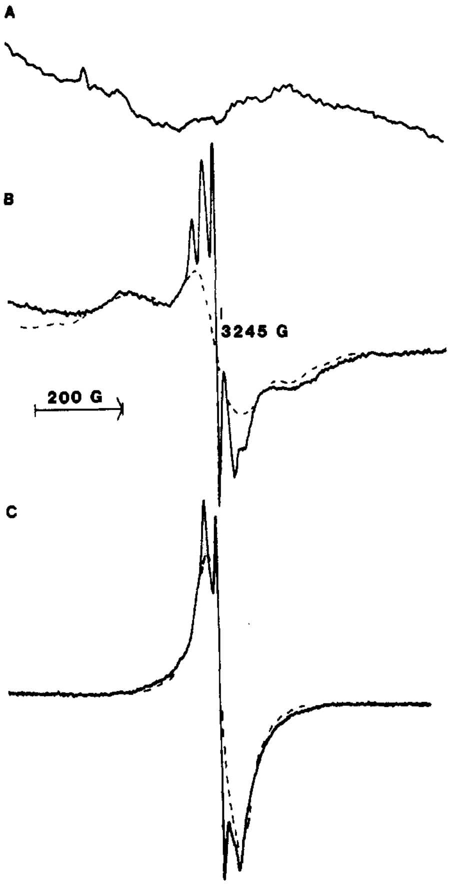

Figure 8. X-Band (9.101 GHz) EPR spectra (1000 G) in frozen solution at −180 °C obtained with 4-G modulation amplitude and 1.0-mW microwave power. (A) Central portion of spectrum of $Mn(EDTA)(H_2O)^{2-}$. (B) Central portion of spectrum of $Mn(EDTA-NO)(H_2O)^-$. The values of the parameters used in the simulation were as follows. Manganese: $g = 2.01$, $D = -0.05$ cm^{-1}, $E/D = 0.333$. Nitroxyl: g values as in Figure 2B. Interaction: $J = -0.004$ cm^{-1}, $r = 8.5$ Å, $\epsilon = 40°$, $\eta = 0°$. (C) Central portion of spectrum of $Mn(EDTA-CH_2-NO)(H_2O)^-$. The values of the parameters used in the simulation were as follows. Manganese: values as in part B. Nitroxyl: g values as in Figure 2B. Interaction: $J = 0.0$ cm^{-1}, $r = 9.5$ Å, $\epsilon = 45°$, $\eta = 0°$. The dotted lines in parts B and C indicate regions in which the simulated spectra do not overlay the experimental curves. The full spectra are extended over about 6000 G.

line widths of about 1.5 G and no resolved spin–spin splitting. Various models for interpreting NMR relaxation data had previously given values of $(1.4-7.3) \times 10^{-12}$ s for T_1 of $Fe(EDTA)(H_2O)^-$.[34] It is therefore probable that the iron relaxation rate was sufficiently fast at room temperature to decouple the iron spin from the nitroxyl spin.

A crystal structure has been reported for a Mn(II) complex of EDTA in which the EDTA is hexadentate and the Mn(II) is 7-coordinate due to coordination of a molecule of water. In the crystal there is also a Mn(II) bound to two carboxylates and four molecules of water.[37] In aqueous solution at pH 4–8 the complex is thought to be $Mn(EDTA)(H_2O)^{2-}$, containing 7-coordinate Mn(II).[18,37,38] The complex of the spin-labeled EDTA derivatives is proposed to be 7-coordinate $Mn(EDTA-NO)(H_2O)_2^-$ although the possibility of 6-coordinate $Mn(EDTA-NO)(H_2O)^-$ is difficult to rule out. It had previously been noted that the ZFS for the Mn(II) complex of EDTA was >150 G[39] (0.014 cm^{-1}). Simulation of the frozen-solution EPR spectra of $Mn(EDTA)(H_2O)^{2-}$ gave D = about 0.05 cm^{-1} and E/D = about $^1/_3$.

In frozen solution the central portion of the EPR spectrum of $Mn(EDTA-NO)(H_2O)_2^-$ had a small signal due to nitroxyl that was not interacting with Mn(II) and some relatively sharp lines near the noninteracting nitroxyl signal, but most of the nitroxyl intensity was in broader lines spread over several hundred gauss (Figure 8B). These broad lines were not present in the spectrum of $Mn(EDTA)(H_2O)^{2-}$ (Figure 8A). The nitroxyl line widths in the simulated spectra were independent of the electron spin of the manganese with which the nitroxyl was interacting, so it was not possible to match the variations in nitroxyl line widths in the experimental spectrum. Since there were two distinctly different line widths in the well-resolved portion of the spectrum, there may be additional broader nitroxyl lines that were shifted further from $g = 2$ and were not resolved from the broad manganese lines. Therefore, the absolute value of J used in the simulation (−0.004 cm^{-1}) can only be regarded as a lower limit. The manganese lines were so broad that no information about the spin–spin interaction was obtained from that portion of the spectrum.

The central portion of the EPR spectrum of $Mn(EDTA-CH_2-NO)(H_2O)_2^-$ in frozen solution is shown in Figure 8C. The spin–spin interaction was markedly weaker than in the spectrum in Figure 8B. The simulated spectrum was obtained with $r = 9.5$ Å and $J = 0.0$. Since the nitroxyl lines gave a broad envelope without resolved features, a variety of orientations of the interspin vector and values of r between 9.0 and 10.0 Å gave comparable agreement with the experimental spectrum. Comparison of the spectra for the complexes of EDTA–NO and EDTA–CH_2–NO indicated that the additional CH_2 group caused a substantial decrease in the spin–spin interaction, as was observed for the complexes with vanadyl, Ni(II), Cr(III), and Fe(III).

In fluid solution the nitroxyl lines in the spectra of $Mn(EDTA-NO)(H_2O)_2^-$ were severely broadened and difficult to distinguish from the more intense manganese lines. The line widths for the nitroxyl signals in $Mn(EDTA-CH_2-NO)(H_2O)_2^-$ were about 20 G, which is similar to the line widths observed for two other spin-labeled Mn(II) complexes with interspin distances about 9 Å.[40] The T_1 value for Mn(II) complexes in fluid solution has been estimated to be $(5-10) \times 10^{-9}$ s.[40,41] This is sufficiently long that the Mn(II) ion would not be decoupled from the nitroxyl.

Complexes of EDTA with the general formula $M(HEDTA)(H_2O)_n$ have been isolated for most of the lanthanides.[42] Complexes with the formula $M(EDTA)(H_2O)_n^-$ have also been found.[43] A crystal structure of $[La(HEDTA)(H_2O)_3]$[44] indicated that the protonated carboxylate was coordinated to La, although the M–O bond was longer than for the deprotonated carboxylates. Thus, the Dy(III) or Gd(III) complexes of EDTA–NO probably had the formula $M(EDTA-NO)(H_2O)_n$ and the amide oxygen may interact with the lanthanide. This could provide a more direct path for spin–spin interaction between the Dy(III) or Gd(III) ion and the nitroxyl than was available in the transition-metal complexes.

In the room-temperature and frozen-solution EPR spectra of the Dy(III) complexes of EDTA–NO and EDTA–CH_2–NO the line shapes of the nitroxyl signals gave no indication of interaction with the lanthanide ion. At room temperature the T_1 value for Dy(III) has been estimated to be about $(3-8) \times 10^{-13}$ s.[45,46] These relaxation times are sufficiently short to decouple the metal from the nitroxyl. Hyde estimated that at −150 °C at X-band $2\pi T_1 \sim 1$ for Dy(III)[47] or T_1 = about 2×10^{-11} s. Consistent with Hyde's observation,[47] Dy(III) had a large impact on the nitroxyl relaxation at −180 °C. The effect was larger for Dy(EDTA–

---

(37) Richards, S.; Pederson, B.; Silverton, J. V.; Hoard, J. L. *Inorg. Chem.* **1964**, *3*, 27.

(38) Zetter, M. S.; Grant, M. W.; Wood, E. J.; Dodgen, H. W.; Hunt, J. P. *Inorg. Chem.* **1972**, *11*, 2701.

(39) Reed, G. H.; Leigh, J. S., Jr.; Pearson, J. E. *J. Chem. Phys.* **1971**, *55*, 3311.

(40) More, J. K.; More, K. M.; Eaton, G. R.; Eaton, S. S. *J. Am. Chem. Soc.* **1984**, *106*, 5395.

(41) McLaughlin, A. C.; Leigh, J. S., Jr.; Cohn, M. *J. Biol. Chem.* **1976**, *251*, 2777.

(42) Kolat, R. S.; Powell, J. E. *Inorg. Chem.* **1962**, *1*, 485.

(43) McConnell, A. A.; Nuttall, R. H.; Stalker, D. M. *Talanta* **1978**, *25*, 425.

(44) Lind, M. D.; Lee, B.; Hoard, J. L. *J. Am. Chem. Soc.* **1965**, *87*, 1611.

(45) Reuben, J.; Fiat, D. *J. Chem. Phys.* **1969**, *51*, 4918.

(46) Burns, P. D.; LaMar, G. N. *J. Magn. Reson.* **1982**, *46*, 61.

(47) Sarna, T.; Hyde, J. S.; Swartz, H. M. *Science (Washington, D.C.)* **1976**, *192*, 1132.

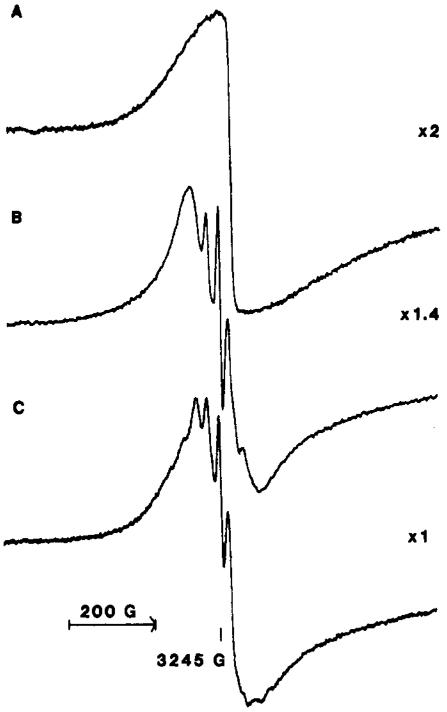

Figure 9. X-Band (9.101 GHz) EPR spectra (1000 G) in frozen solution at −180 °C: (A) spectrum of Gd(EDTA)$(H_2O)_n^-$ obtained with 2-G modulation amplitude and 0.2-mW microwave power; (B) spectrum of Gd(EDTA–NO)$(H_2O)_n$ obtained with 2-G modulation amplitude and 0.2-mW microwave power; (C) spectrum of Gd(EDTA–CH_2–NO)$(H_2O)_n$ obtained with 4-G modulation amplitude and 0.2-mW microwave power. The relative amplification of the spectra was corrected for differences in spectrometer settings and sample concentration.

NO)$(H_2O)_n$ than for Dy(EDTA–CH_2–NO)$(H_2O)_n$, which is consistent with a significant exchange interaction in the EDTA–NO complex.

Metal with $S = {}^7/_2$, Gadolinium(III). The EPR spectrum of the Gd(III) complex of EDTA in frozen solution is shown in Figure 9A. In the center of the spectra of Gd(EDTA–NO)$(H_2O)_n$ (Figure 9B) and Gd(EDTA–CH_2–NO)$(H_2O)_n$ (Figure 9C) there was a small sharp signal due to nitroxyl that was not interacting with the Gd(III). However, in both of the spectra most of the nitroxyl intensity was in lines that were split due to interaction with the Gd(III) unpaired electrons. The spectrum of Gd(EDTA–CH_2–NO)$(H_2O)_n$ can be regarded as the superposition of a split nitroxyl signal on top of a largely unchanged Gd(III) signal. In the spectrum of Gd(EDTA–NO)$(H_2O)_n$ both the nitroxyl and the Gd(III) signals appear to have been substantially altered by the spin–spin interaction. It would appear that the spin–spin interaction was substantially greater for the complex of EDTA–NO than for the complex of EDTA–CH_2–NO.

In the fluid-solution EPR spectra of Gd(EDTA–NO)$(H_2O)_n$ and Gd(EDTA–CH_2–NO)$(H_2O)_n$ the nitroxyl signals were superimposed on the broader Gd(III) signals. The line widths for the nitroxyl signals in the fluid-solution spectra of Gd(EDTA–NO)$(H_2O)_n$ and Gd(EDTA–CH_2–NO)$(H_2O)_n$ were 60 and 17 G, respectively. Although resolved spin–spin splitting was not observed, the larger line widths of the nitroxyl signals for the complex of EDTA–NO than for the complex of EDTA–CH_2–NO indicated substantially greater spin–spin interaction for the former than for the latter, which is consistent with the results obtained in frozen solution. The T_1 value for Gd(III) complexes in fluid solution at room temperature has been estimated to be between 10^{-9} and 10^{-10} s.[48,49] These values suggest that splittings due to spin-spin interaction could be partially collapsed by the metal relaxation. The observation of nitrogen hyperfine splitting in the EPR spectrum of gadolinium(III) myoglobin[50] together with our results on spin-labeled porphyrins[51] suggest that exchange interactions involving Gd(III) may be more important than previously recognized.

Effect of Metal *S* on the Value of *J*. If the geometry of a series of complexes remains constant and the electron–electron spin–spin interaction is via a single d orbital, the magnitude of the exchange interaction is expected to be inversely proportional to the number of unpaired electrons.[52] Consistent with this model, exchange interactions in metal dimers and in spin-labeled vanadyl and Mn(II) complexes tend to decrease as the number of unpaired electrons increases.[40,53–57] It should also be noted that if more than one unpaired electron on the metal is involved in the exchange interaction, the two contributions to J may be of opposite sign. Thus, smaller than expected values could also be the result of near cancellation of two terms.

The value of J was smaller for the Cr(III) complex ($S = {}^3/_2$, $|J| = 0.006–0.008\ \text{cm}^{-1}$) than for the vanadyl complex ($S = {}^1/_2$, $|J| = 0.014\ \text{cm}^{-1}$). Due to the low symmetries of the complexes the geometries may be different. In the vanadyl complex the unpaired electron is presumably in the d_{xy} orbital (directed between the M–L bonds). In the Cr(III) complex the d_{xy}, d_{xz}, and d_{yz} orbitals each contain one unpaired electron. The primary contribution to the metal–nitroxyl interaction is probably through one of these orbitals although there may be some interaction with a second unpaired electron. Thus, the observation of about a factor of 2 decrease instead of a factor of 3 decrease in the values of J from vanadyl to Cr(III) is in general agreement with the model.

The value of J for the Fe(III) complex ($S = {}^5/_2$, $|J| = 0.013\ \text{cm}^{-1}$) was about the same as for the vanadyl complex ($S = {}^1/_2$, $|J| = 0.014\ \text{cm}^{-1}$). In the Fe(III) complex each of the d orbitals contains an unpaired electron. Even in the low-symmetry 7-coordinate complex it is probable that overlap with d_{z^2} or $d_{x^2-y^2}$ would give a more effective pathway for exchange interaction than is possible in the vanadyl and Cr(III) complexes. Thus, the assumption that the interaction is via the same d orbital probably does not hold for the comparison of vanadyl and Fe(III) and the dependence on the number of unpaired electrons is not expected.

Effect of Metal Relaxation on the Nitroxyl EPR Spectra. At −180 °C resolved spin–spin splitting was observed in the spectra of the complexes of EDTA–NO with Cu(II), vanadyl, Cr(III), Fe(III), Mn(II), and Gd(III), which is consistent with the expectation that the relaxation times for these metals at this temperature are long relative to the magnitude of the spin–spin interactions. The lines in the spectra of the Ni(II) complex were severely broadened, which suggested that the splittings were partially collapsed by relaxation of the nickel unpaired electrons. The relaxation time of Dy(III) was so short that spin–spin splittings were fully collapsed.

In fluid solution the relaxation times for Fe(III), Ni(II), and Dy(III) were sufficiently short to fully collapse the spin–spin splitting of the nitroxyl by the metals. Broadened nitroxyl lines were observed for the EDTA–NO complexes of Mn(II), Cr(III), Cu(II), and Gd(III), which is consistent with slower relaxation rates for these metals than for Fe(III), Ni(II), or Dy(III). Since the dominant contribution to the spin–spin interaction for the Cu(II) complex in frozen solution was dipolar and dipolar splitting is largely averaged out by molecular tumbling, spin–spin splitting would not be expected in the fluid-solution spectra of the Cu(II) complexes. The observation of broadened lines instead of resolved spin–spin splittings for the four other metals could indicate that

---

(48) Dwek, R. A.; Levy, H. R.; Radda, G. K.; Seeley, P. J. *Biochim. Biophys. Acta* **1975**, *377*, 26.

(49) Hyde, J. S.; Sarna, T. *J. Chem. Phys.* **1978**, *68*, 4439.

(50) Srivastava, T. S. *Curr. Sci.* **1980**, *49*, 429.

(51) More, K. M.; Eaton, S. S.; Eaton, G. R. *J. Am. Chem. Soc.* **1981**, *103*, 1087.

(52) Hay, P. J.; Thibeault, J. C.; Hoffmann, R. *J. Am. Chem. Soc.* **1975**, *97*, 4884.

(53) Lambert, S. L.; Hendrickson, D. N. *Inorg. Chem.* **1979**, *18*, 2683.

(54) Spiro, C. L.; Lambert, S. L.; Smith, T. J.; Duesler, E. N.; Gagne, R. P.; Hendrickson, D. N. *Inorg. Chem.* **1981**, *20*, 1229.

(55) Torihara, N.; Okawa, H.; Kida, S. *Chem. Lett.* **1978**, 185.

(56) O'Connor, C. J.; Freberg, D. P.; Sinn, E. *Inorg. Chem.* **1979**, *18*, 1077.

(57) Lambert, S. L.; Spiro, C. L.; Gagne, R. R.; Hendrickson, D. H. *Inorg. Chem.* **1979**, *18*, 1077.

the metal relaxation time was comparable to the magnitude of the splitting (partial collapse of the splitting) or that flexibility of the molecules in fluid solution caused uncertainty in the magnitude of the exchange interaction. Resolved spin–spin splitting was observed for the vanadyl complex of EDTA–NO, which is consistent with slow relaxation of the vanadyl unpaired electron.

Conclusions

Resolved spin–spin splitting was observed in the frozen-solution EPR spectra of the Cu(II), vanadyl, Fe(III), Mn(II), and Gd(III) complexes of EDTA–NO. The small differences between the spectra of the Cu(II) complexes of EDTA–CH$_2$–NO and EDTA–NO indicated that the spin–spin interaction in both complexes was primarily dipolar. The large differences in the spectra of the EDTA–NO and EDTA–CH$_2$–NO complexes of vanadyl, Ni(II), Fe(III), Mn(II), and Gd(III) indicated that there was a substantial exchange contribution to the interaction in the EDTA–NO complexes that was greatly attenuated in the EDTA–CH$_2$–NO complexes.

Acknowledgment. This work was supported in part by NIH Grant GM21156. S.S.E. thanks the NSF for a Visiting Professorship for Women, 1984. Professor Belford provided a copy of his fourth-order frequency shift subroutine and helpful comments concerning its use. Dr. Dragutan (Romania) and Professor Hideg (Hungary) provided useful information concerning the synthesis of compound IV. Professor Dervan provided a preprint of the experimental section of ref 6. EI mass spectra were obtained at the Midwest Center for Mass Spectrometry at the University of Nebraska, supported under the National Science Foundation Regional Instrumentation Facilities Program. FAB mass spectra were obtained at the Mass Spectrometry Research Resource at the University of Colorado Health Science Center, which receives partial support from NIH Division of Research Resources, Grant RR01152.

Registry No. I, 102587-64-4; II, 102587-65-5; III, 102587-66-6; IV, 56674-44-3; Et$_3$–EDTA–NO, 102587-67-7; Li$_3$–EDTA–NO, 102587-68-8; Et$_3$–EDTA–CH$_2$–NO, 102587-69-9; Li$_3$–EDTA–CH$_2$–NO, 102587-70-2; Cu(HEDTA–NO)(H$_2$O), 102538-91-0; Cu(HEDTA–CH$_2$–NO)(H$_2$O), 102538-92-1; VO(EDTA–NO)$^-$, 102538-93-2; VO(EDTA–CH$_2$–NO)$^-$, 102538-94-3; Ni(HEDTA–NO)(H$_2$O), 102538-95-4; Ni(HEDTA–CH$_2$–NO)(H$_2$O), 102538-96-5; Cr(EDTA–NO)(H$_2$O), 102538-97-6; Cr(EDTA–CH$_2$–NO)(H$_2$O), 102538-98-7; Fe(EDTA–NO)(H$_2$O)$_2$, 102538-99-8; Fe(EDTA–CH$_2$–NO)(H$_2$O)$_2$, 102539-00-4; Mn(EDTA–NO)(H$_2$O)$_2$, 102539-01-5; Mn(EDTA–CH$_2$–NO)(H$_2$O)$_2$, 102539-02-6; Cu(H$_2$EDTA)(H$_2$O), 24778-06-1; Cu(HEDTA)$^-$, 102539-03-7; VO(EDTA)$^{2-}$, 20648-98-0; Cr(HEDTA)(H$_2$O), 76582-41-7; Mn(EDTA)(H$_2$O)$^{2-}$, 38702-75-9; triethyl ethylenediaminetetraacetate, 90359-20-9; 4-amino-2,2,6,6-tetramethylpiperidinyl-1-oxy, 14691-88-4; 4-(hydroxymethyl)-2,2,6,6-tetramethylpiperidinyl-1-oxy, 61546-66-5.

Contribution from Analytical and Radiochemistry,
University of Liège, Sart Tilman (B6), B-4000 Liège, Belgium

Coordination of Lanthanides by Two Polyamino Polycarboxylic Macrocycles: Formation of Highly Stable Lanthanide Complexes

M. F. Loncin, J. F. Desreux,* and E. Merciny

Received December 6, 1985

The formation constants of a few lanthanide complexes with DOTA (1,4,7,10-tetraazacyclododecane-*N,N′,N″,N‴*-tetraacetic acid) and TETA (1,4,8,11-tetraazacyclotetradecane-*N,N′,N″,N‴*-tetraacetic acid) have been measured by potentiometric and competition methods. The ligand DOTA forms the most stable lanthanide chelates known so far (log K_{ML} = 28.2–29.2) while the stability of the TETA compounds at 80 °C (log K_{ML} = 14.5–16.5) is comparable to the stability of the EDTA complexes. A competition method with the oxalate anion as a probe had to be used for determining the formation constants of the DOTA lanthanide chelates because of the high stability of these compounds. The relative stability of the DOTA and TETA complexes in accounted for by steric factors with reference to known solution- and solid-state structures.

Introduction

The lanthanide complexes with polyaza polycarboxylic macrocycles such as 1,4,7,10-tetraazacyclododecane-*N,N′,N″,N‴*-tetraacetic acid, DOTA (**1**), or 1,4,8,11-tetraazacyclotetradecane-*N,N′,N″,N‴*-tetraacetic acid, TETA (**2**), display a host of

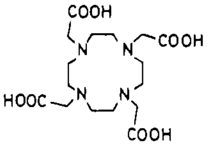

1

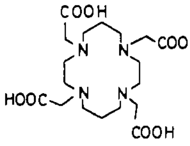

2

unusual properties that are not exhibited by the complexes of similar but noncyclic ligands such as EDTA or DTPA. The DOTA and TETA lanthanide chelates are remarkably rigid, they are highly symmetric, and they adopt the same geometry in solution and in the solid state.[1-4] This lack of lability is most unusual in lanthanide chemistry[5] and has been assigned to the steric requirements of the 12- and 14-membered cycles. The results of recent efforts at determining reliable stability constants of a few lanthanide DOTA and TETA complexes are reported in this paper. Particularly worthy of note is the very high stability of the DOTA compounds that are by far the most stable lanthanide complexes known to date. Their high stability could turn out to be especially important in two very different areas of research where inert complexes are potentially useful, namely for the separation of the lanthanides as a class of metals and for the design of Gd(III) contrast agents for NMR imaging.[6]

Experimental Section

Materials and Standard Solutions. The syntheses of DOTA and TETA followed previously reported procedures.[1,4] Stock solutions of the ligands were analyzed by potentiometric titration with sodium hydroxide, and stock solutions of metal chlorides or perchlorates were standardized by EDTA titration. Carbonate-free NaOH solutions were used to adjust the pH of the solutions to the desired values.

Solutions of the DOTA and TETA lanthanide complexes were prepared either by direct dissolution of a stoichiometric quantity of a metal oxide into a standardized solution of the ligand at 80 °C or by slowly

---

(1) Desreux, J. F. *Inorg. Chem.* **1980**, *19*, 1319–1324.
(2) Spirlet, M. R.; Rebizant, J.; Desreux, J. F.; Loncin, M. F. *Inorg. Chem.* **1984**, *23*, 359–363.
(3) Spirlet, M. R.; Rebizant, J.; Loncin, M. F.; Desreux, J. F. *Inorg. Chem.* **1984**, *23*, 4278–4283.
(4) Desreux, J. F.; Loncin, M. F. *Inorg. Chem.* **1986**, *25*, 69–74.
(5) See for instance: Richardson, F. S. *Chem. Rev.* **1982**, *82*, 541–552. Greenwood, N. N.; Earnshaw, A. In *Chemistry of the Elements*; Pergamon: New York, 1984; p 1434.
(6) Weinman, H.-J.; Brasch, R. C.; Press, W.-R.; Wesbey, G. E. *Am. J. Roentgenol.* **1984**, *142*, 619–624.

0020-1669/86/1325-2646$01.50/0